Kinetics and Catalysis, Vol. 45, No. 5, 2004, pp. 628–633. Translated from Kinetika i Kataliz, Vol. 45, No. 5, 2004, pp. 668–673.

Kinetics of Thermal Decomposition and Oxidation of Soot Particles in Shock Waves

P. A. Vlasov, Yu. K. Karasevich, and V. N. Smirnov

Semenov Institute of Chemical Physics, Russian Academy of Sciences, Moscow, Russia

Received December 25, 2002

Abstract—A new method was proposed for studying the kinetics of gas-dispersed systems in shock waves. The method is based on the pulsed sputtering of microscopic amounts of finely grained powder immediately before arrival of a shock wave. The method was used for investigating the oxidation of soot particles with molecular hydrogen (T = 1700–2400 K) and their vaporization (T = 4000–6000 K) in an argon atmosphere. The rates of these processes and the time dependence of the temperature of soot particles were measured. A model was proposed for characterizing the vaporization of soot.

INTRODUCTION

The thermal decomposition and oxidation of soot are of scientific and practical interest [1–3]. Shock-wave tubes are particularly attractive for modeling these processes owing to the possibility of the uniform heating of large volumes of gases (gas-dispersion media) in a wide range of temperatures and pressures (T = 500–10000 K, P = 0.1–100 atm). The shock-wave technique is efficient for investigating thermal processes (relaxation of different degrees of freedom, chemical reactions, and ionization) in homogeneous systems [4]. However, the use of shock waves for investigating high-temperature processes in gas-dispersion media involves difficulties. First, it is necessary to create a sufficiently homogeneous distribution of heterogeneous particles in the test gas-dispersion medium. Second, it is necessary to determine the parameters of shock waves in gas-dispersion mixtures.

In this work, a new method for preparing gas-dispersion media in a shock-wave tube is described, and results of a study of soot vaporization and oxidation using this method are reported.

EXPERIMENTAL

A shock-wave tube 76 mm in bore with low- and high-pressure chambers 3.2 and 1.5 m long was used. Before each experiment, the low-pressure chamber was evacuated out to a pressure of 10^{-3} Torr using a diffusion pump combined with a fore (rotary vane) pump and additionally washed with pure argon.

A device designed for this method is schematically depicted in Fig. 1. The essentials of the device are the following: a pneumatic piston unit with a capacity of 2 ml (*1*), a socket for mounting the device at the end face of the tube (*2*), a polyethylene membrane (*3*), and a percussion trigger mechanism (*4*). A spreading disk (*5*) (3 mm in diameter mounted at a distance of 2 mm from the end face of the tube) serves to gain better dispersion of particles and more homogeneous particle distribution over the tube. Particles were injected into the shock-wave tube using a sprayer as described below. The dispersing device was filled with a working gas (argon or its mixture with oxygen, depending on the aim of the experiment) through a rubber septum. Then, the beak of the device was dropped into a layer of soot 1.5–2 mm thick. As a result, the beak was filled with the powder to a height approximately equal to the layer thickness (3–5 mg). In some experiments, soot was partially removed by lightly tapping the beak. In this case,

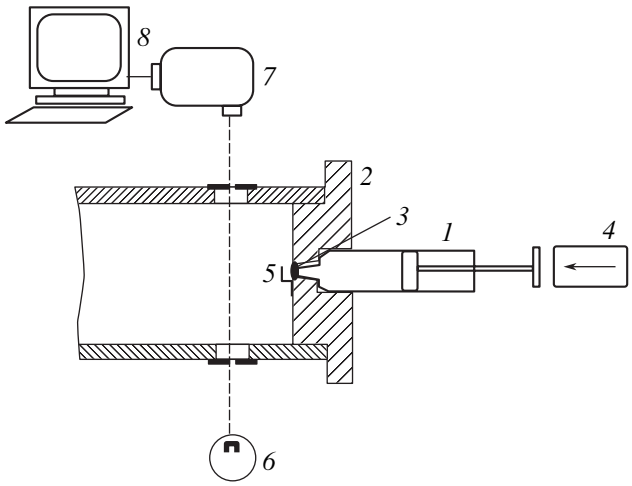

Fig. 1. Schematic diagram of the setup: (*1*) pneumatic piston device with a capacity of 2 ml; (*2*) mounting socket at the end face of the tube; (*3*) polyethylene membrane; (*4*) percussion trigger mechanism; (*5*) spreading disk; (*6*) tungsten ribbon lamp SI-10-300; (*7*) monochromator; and (*8*) data acquisition, storage, and processing system. The probe beam of the absorption channel (not shown) is directed at a right angle to the plane of the figure.

0023-1584/04/4505-0628 © 2004 MAIK "Nauka/Interperiodica"

1.5–2.5 mg of the powder was retained on the beak walls. Then, polyethylene film *3* was placed between the device and the socket, and the device was inserted into the socket. In this case, the polyethylene membrane served as a vacuum seal between the socket and the beak of the device, which kept atmospheric air from entering the shock-wave tube. To gain a tighter seal, the film was coated on the socket side with a thin layer of vacuum grease. The tube was evacuated out, washed, and filled with the test gas mixture. Then, we started to raise the pressure of the driver gas (helium) in the high-pressure section. Two to three seconds before the membrane separating the high- and low-pressure sections of the shock-wave tube was broken, the percussion trigger mechanism (a percussion hammer) was activated. The hammer hit the piston, which compressed the gas in the device. As a result, the polyethylene membrane was broken, and soot was dispersed inside the tube.

Special measurements showed that the gas-dispersion cloud occupied a volume of about one liter and extended for a distance of 20 cm from the end face of the shock-wave tube. In this case, at a distance of 5–12 cm from the end face, the particle density was constant and decreased in both directions from this range. At typical gas pressures in the low-pressure chamber (30–40 Torr), the characteristic time of settling of soot particles was 20–30 s. This time was measured by a decrease in light adsorption by the gas-dispersion medium. Thus, in the 2–3 s period between the dispersion of the powder and the breakage of the membrane generating the shock wave soot did not settle noticeably on the walls of the shock-wave tube.

The test soot was synthesized by the oxidation of methane in rich mixtures with air ($\phi = 2.5$) in shock waves. Soot particles dispersed in a shock-wave tube at $P_{Ar} = 30$ Torr and then deposited on a copper support were investigated using a scanning electron microscope. The investigation showed that individual soot particles had a near-spherical shape with an average radius of ~20 nm. Approximately half the total amount of particles was associated in agglomerates of 3–5 individual particles; that is, with the sputtering method described above, the powder was not dispersed entirely. In an analogous study of deposited soot subjected to (incident and reflected) shock waves, it was found that the sample was composed dominantly of individual particles. Hence, it is likely that agglomerates were broken down in the shock front. Thus, it is believed that the gas-dispersion medium behind the reflected shock wave is composed of individual particles. The same conclusion was made in [2].

In this work, the emission from and absorption by a gas-dispersion medium at 530 nm were measured simultaneously at the same section at a distance of 10 mm from the end face of the shock-wave tube (the two-beam method) [5]. The measuring scheme is illustrated in Fig. 1. The measurements of the time dependence of absorption and emission provide a means of determining the true or effective temperature of the gas (gas-dispersion) medium in equilibrium or nonequilibrium conditions, respectively. The calculation procedure was described in detail in [6]. With a gas phase transparent to emission at the operating wavelength, the calculated temperature refers to particles. This is the case in this work because oxygen and argon do not absorb in the visible spectrum.

RESULTS AND DISCUSSION

Typical absorption and emission curves and the calculated time dependence of the temperature for the thermal decomposition of soot particles behind the shock wave in argon are presented in Fig. 2. The emitted intensity is given with reference to the emission from a SI-10-300 tungsten filament lamp with a dc source of 24 A. It is seen that the temperature of soot particles steeply rises (during their heating), reaches a maximum, and then gradually decreases. In all cases, even when soot particles were not vaporized (absorbance was virtually constant), the measured temperature of soot particles was below the temperature of the gas behind the shock wave. The temperature of the gas (argon) was calculated in terms of conservation laws from the data [7]. The temperature difference was found to be nearly proportional to the calculated temperature: ~200 K for 2000 K and ~300 K for 3000 K. The vaporization of particles occurred at a calculated gas temperature of ~4000 K. In this case, the difference between the calculated temperature of the gas and the measured temperature of the particles was greater than that in the absence of vaporization and further increased with the rate of vaporization.

In the absence of particle vaporization, the difference between the calculated temperature and the temperature determined from optical measurements can be explained by gas-dynamic and heat effects: the shock wave propagating in pure argon is partially reflected from the gas-dispersion cloud with a loss of the kinetic energy of the gas. Moreover, the particles contribute to the heat capacity of the gas-dispersion medium, which also decreases the temperature as compared with the temperature calculated for pure argon from the measured shock wave velocity. The calculation of parameters of the gas-dispersion medium behind shock waves is a rather complex problem; therefore, the temperature determined from optical measurements was taken as the temperature behind the shock wave.

The vaporization and oxidation of particles additionally complicated the determination of the temperature and other parameters of the gas-dispersion medium behind shock waves. Therefore, in the range $T = 1700$–3000 K, the initial temperature of the gas-dispersion medium behind the shock front was estimated by the dependence of the temperature determined from optical

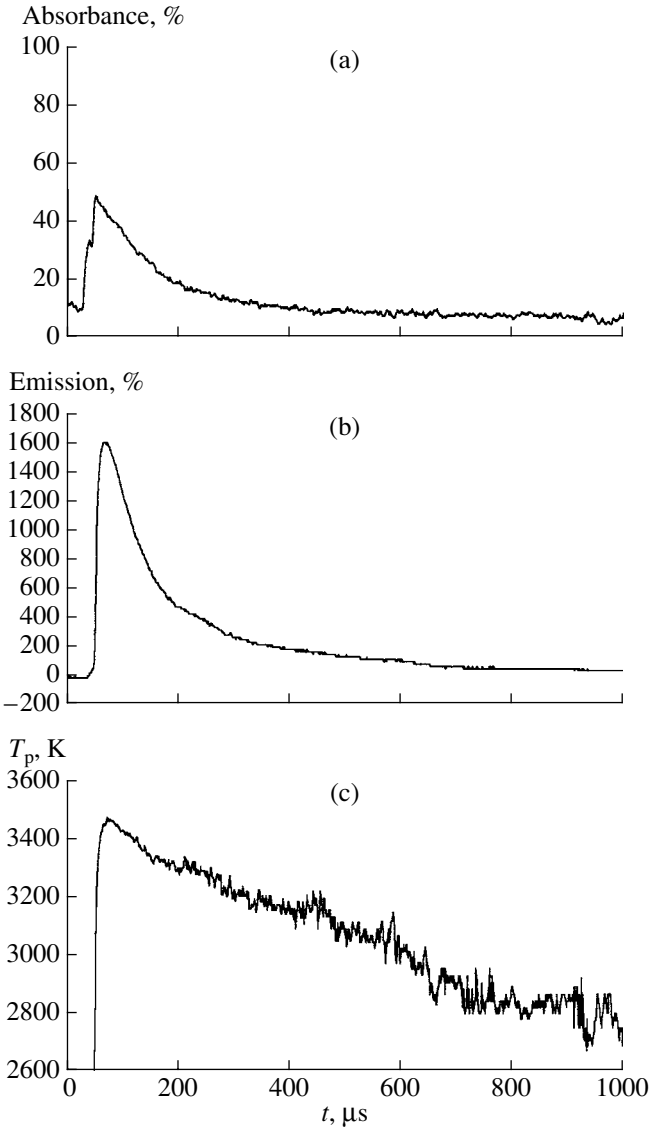

Fig. 2. (a) Absorption and (b) emission oscillograms of the gas-dispersion medium and (c) the time dependence of the effective temperature of soot particles calculated from the oscillograms (see the text). The gas temperature calculated from the shock wave velocity in pure argon is equal to 4290 K; the gas temperature estimated as described in the text is equal to 3870 K.

measurements on the temperature calculated from the shock wave velocity in argon, in conditions when neither combustion of the particles nor their vaporization occurred. In the temperature range above 3000 K, which corresponds to the thermal decomposition of the particles, a linear extrapolation of this dependence was used.

The vaporization or oxidation of soot particles decreased both absorption by the particles and emission from them. Microscopic studies showed that the maximum of the particle size distribution corresponded to an average radius of about 20 nm. With the distribution function recommended for different kinds of soot [8], this corresponds to the characteristic radius of the distribution $R_c \approx 10$ nm. Since the particles are much smaller than the wavelength in the absorption measurements (the Rayleigh absorption regime), in accordance with the Mie theory [9], the absorbance is proportional to the mass of condensed particles in a unit volume. Consequently, the observed decrease in the absorbance is due to the decrease in the mass of soot particles in their vaporization or oxidation. The kinetics of these processes was described in terms of the rate of mass loss from unit surface area of the particles in unit time ω, g cm^{-2} s^{-1}. The values of ω were determined from oscillograms of light absorption by the gas-dispersion medium using nomograms constructed under the assumption that the particle size distribution represents an asymmetric Gaussian distribution [8]. These nomograms are of the form

$$\frac{D(\tau)}{D_{max}} = \frac{\int_{\tau^2}^{\infty}(x^{1/2}-\tau)^3\exp(-x)dx}{\int_0^{\infty}x^{3/2}\exp(-x)dx}, \quad (1)$$

where $D(\tau)$ is the running absorbance; D_{max} is the maximum absorbance at the shock front ($t = 0$); $x = (R/R_c)^2$; R (cm) is the running particle radius; $\tau = \omega t/\rho R_c$ is the dimensionless time; ρ (g/cm^3) is the density of the material of soot particles; and t (s) is the running time. The values of ω were chosen so that the experimental $D(\tau)/D_{max}$ function fit the theoretical function. The determination of the parameter ω is illustrated in Fig. 3 with the experiment presented in Fig. 2.

The dependence of the vaporization rate on the measured effective temperature of particles is presented in Fig. 4. Also shown is the temperature dependence of the vaporization rate for graphite, which was calculated from the tabulated values of vapor pressure over graphite [7]. The calculation was carried out under the assumption that the accommodation (adhesion) coefficient of the carbon atom in its collision with the graphite surface is equal to unity. It is seen that the experimental data are in sufficiently good agreement with the calculated values.

As already mentioned, the decomposition of particles is accompanied by a decrease in their temperature due to heat losses by vaporization. As a result, the temperature of the particles differs from the temperature of the gas. An analogous phenomenon was observed in the vaporization of iron clusters [5, 6]. The difference in temperature between the particles and the gas can be described in terms of a simple model based on the assumption that the energy lost by the particle through vaporization is compensated due to its collisions with

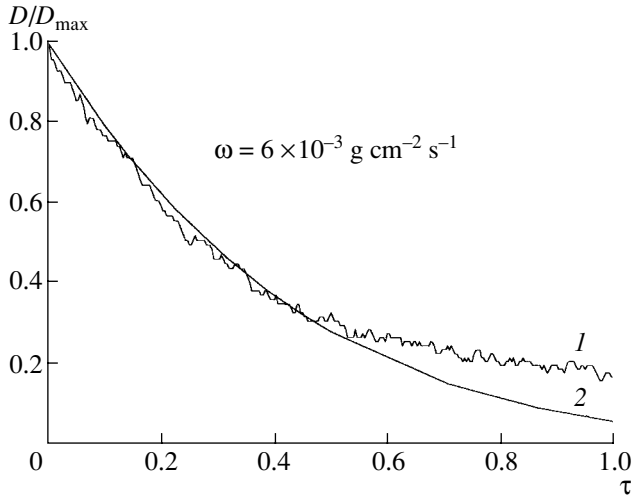

Fig. 3. Calculation of the vaporization rate of soot particles by fitting (*1*) the measured absorbance profile to (*2*) the theoretical profile in dimensionless coordinates.

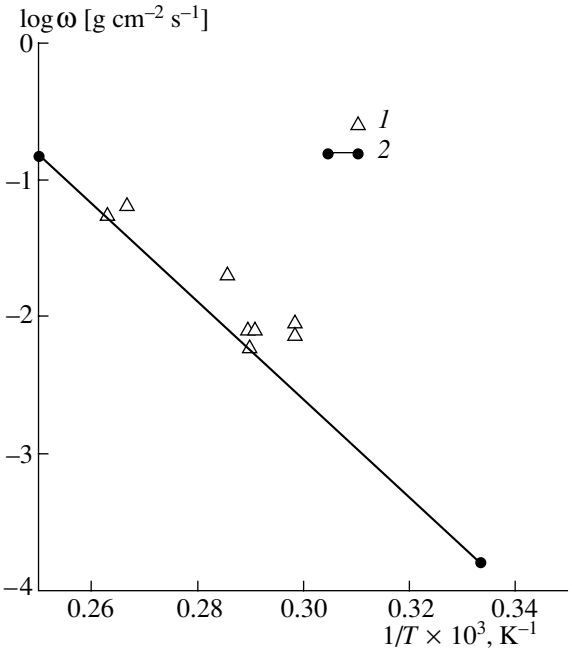

Fig. 4. (*1*) Dependence of the vaporization rate of soot particles on the measured temperature of the particles and (*2*) the calculated temperature dependence of the vaporization rate of graphite (see the text).

surrounding gas molecules; that is, energy fluxes corresponding to these processes are equal to each other. For simplicity, the back process of attachment of carbon atoms to the particles and the energy lost in ionization and emission are ignored in the model. The Monte Carlo simulation [10] of the decomposition of iron clusters showed that the influence of these processes on the energy state of particles at high temperatures is small compared to their vaporization. To test the validity of this model, we correlated the rates of vaporization calculated by the model with rates determined from absorbance profiles by the procedure described above.

In our experiments, soot particles were much smaller than the free path length of diluent gas molecules, and the process of energy transfer was controlled by the rate of energy transfer in collisions of the molecules with the particle surface [11]. This rate can be represented as

$$w_{\text{col}} = \alpha Z_{\text{col}}[\text{M}]C_v(T_\text{g} - T_\text{p}), \qquad (2)$$

where α is the thermal accommodation coefficient; Z_{col} (s^{-1}) is the collision frequency of gas molecules with the particle; [M] (cm^{-3}) is the concentration of diluent gas molecules; C_v is the heat capacity at constant volume for diluent gas molecules ($C_v = 3/2k$; k (J/K) is the Boltzmann constant); and T_g and T_p are the temperatures of the gas and particles, respectively.

The rate of heat loss by a particle through vaporization is expressed as

$$w_{\text{vap}} = 4\pi R^2 \omega \Delta H_{\text{vap}}/\mu_\text{C}, \qquad (3)$$

where R is the particle radius, ω is the vaporization rate, ΔH_{vap} is the heat of vaporization of graphite, and μ_C is the atomic weight of carbon. Equating (2) and (3) and taking into account that $Z_{\text{col}} = \pi R^2 v_{\text{Ar}}$, where v_{Ar} is the mean thermal velocity of diluent gas (argon) atoms, we obtain the following expression for ω:

$$\omega = \frac{3}{8}\alpha\mu_\text{C} v_{\text{Ar}} k(T_\text{g} - T_\text{p})[\text{M}]/\Delta H_{\text{vap}}. \qquad (4)$$

According to [11], the thermal accommodation coefficient can be approximately calculated by the formula

$$\alpha \cong 2.4(\mu_{\text{Ar}}/\mu_\text{C})/(1 + \mu_{\text{Ar}}/\mu_\text{C})^2 = 0.42,$$

where μ_{Ar} is the atomic weight of argon.

The ratio of the vaporization rate ω_T calculated by Eq. (4) from the measured temperature of soot particles and the temperature of the gas determined as described above to the rate of vaporization of the particles ω_A calculated from the time dependence of the absorbance are presented in Fig. 5. It can be seen that the rates of vaporization of soot determined by the two methods agree to within a factor of 2 (a typical scatter for kinetic measurements in shock waves). This indicates that the proposed model is realistic. The observed discrepancy can be explained by errors in the measurement of the temperature of particles and in the determination of the temperature of the gas, by ignoring the back process of

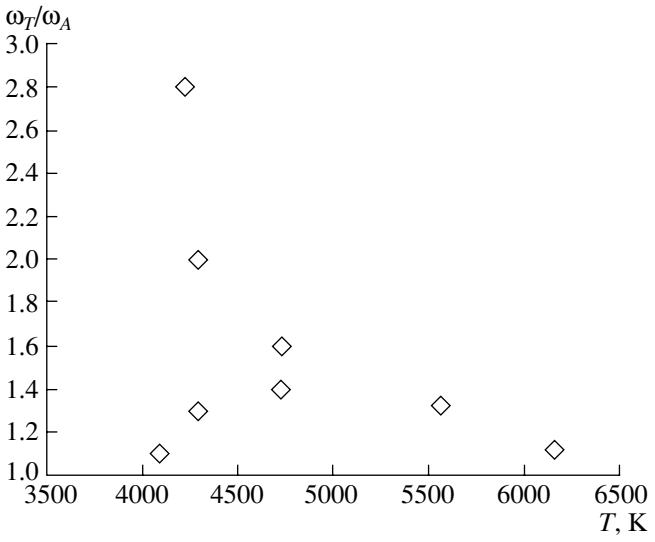

Fig. 5. Ratio of the vaporization rate of soot particles calculated by Eq. (4) from the measured temperature of the particles (ω_T) to the vaporization rate determined from the absorbance profile (ω_A).

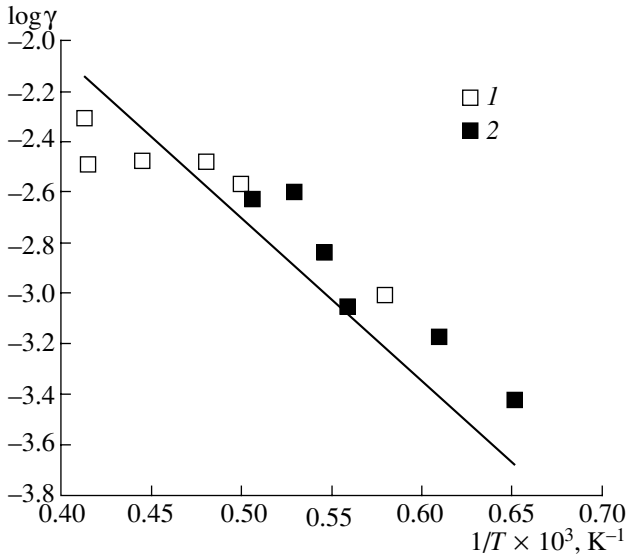

Fig. 6. The temperature dependence of the probability of oxidation of soot particles with O_2–Ar mixtures at O_2 concentrations of (*1*) 20 and (*2*) 50%. The total density of the gas mixture is 2.0×10^{-5} mol/cm^3. The solid line indicates averaged data from [2, 8, 12].

attachment of carbon atoms to the particles and the energy lost by the particles in ionization and emission, and also by deviation of the particle distribution from the asymmetric Gaussian distribution, which was used in this work.

The oxidation of soot with molecular oxygen in a gas phase was studied extensively in the last 30–40 years (see [1] and references therein). In this work, the oxidation of soot particles with molecular oxygen in argon was studied in the temperature range 1720–2420 K at oxygen concentrations of 20 and 50%. The oscillograms of optical absorption and emission were similar in shape to those for the vaporization of soot. We were the first to measure the effective temperature of particles during their oxidation. A comparison of this temperature with the temperature measured in experiments with equivalent amounts of nitrogen instead of oxygen showed that, in oxidation, the temperature of particles is 100–200 K higher than the temperature of the diluent gas. This means that the heat evolved in the exothermic process at the particle surface is transferred, if only in part, to the particle. According to [12], this process is

$$2C_s + O_2 = 2CO.$$

The heat of the overall reaction is equal to ~220 kJ/mol. The observed difference in temperature between the particles and the diluent gas can be qualitatively explained under the assumption that the energy evolved in the oxidation process goes entirely into the heating of particles. This value can be estimated by Eq. (4) with the heat of oxidation of carbon in place of ΔH_{vap}.

The temperature dependence of the probability of oxidation of soot particles γ is presented in Fig. 6. This probability is determined as the number of acts of oxidation of carbon atoms on unit surface area of the particle in unit time divided by the number of collisions of oxidant (oxygen) molecules with the same surface in the same time. For comparison, we plotted averaged data from [2, 8, 12], which agree with each other and, as is seen, with the results of this work.

Thus, the new method proposed for investigating gas-dispersion mixtures in shock waves was tested in the vaporization and oxidation of soot. The rate of vaporization of prepared soot behind shock waves was measured for the first time. The results on the oxidation of soot particles with molecular oxygen are in good agreement with published data. This suggests that the proposed method is efficient, and it can be used for investigating other gas-dispersion systems.

ACKNOWLEDGMENTS

This work was supported by the Russian Foundation for Basic Research, project nos. 01-03-32034 and 02-03-04002-NNIO.

REFERENCES

1. *Soot Formation in Combustion*, Bockhorn, H., Ed., Berlin: Springer, 1994.

2. Cadman, P. and Denning, R.J., *J. Chem. Soc., Faraday Trans.*, 1996, vol. 92, no. 21, p. 4159.
3. Higgins, K.J., Jung, H., Kittelson, D.B., Roberts, J.T., and Zachariah, M.R., *J. Phys. Chem. A*, 2002, vol. 106, p. 96.
4. Zaslonko, I.S., *Usp. Khim.*, 1997, vol. 66, no. 6, p. 537.
5. Vlasov, P.A., Zaslonko, I.S., Karasevich, Yu.K., and Smirnov, V.N., *Khim. Fiz.*, 1988, vol. 8, no. 3, p. 370.
6. Vlasov, P.A., Karasevich, Yu.K., and Smirnov, V.N., *Teplofiz. Vys. Temp.*, 1997, vol. 35, no. 2, p. 200.
7. *JANAF Thermochemical Tables, Phys. Chem. Ref. Data*, 1985, vol. 14, suppl. 1.
8. Park, C. and Appleton, J.P., *Combust. Flame*, 1973, vol. 20, p. 369.
9. Petrov, Yu.I., *Klastery i malye chastitsy* (Clusters and Small Clusters), Moscow: Nauka, 1986.
10. Vlasov, P.A., Karasevich, Yu.K., and Smirnov, V.N., *Teplofiz. Vys. Temp.*, 1996, vol. 34, no. 5, p. 676.
11. Goodman, F.O., *J. Phys. Chem.*, 1980, vol. 84, no. 12, p. 1431.
12. Brandt, O. and Roth, P., *Combust. Flame*, 1989, vol. 77, p. 69.